Significantly Improved Resolution for NOE Correlations from Valine and Isoleucine ($C^{\gamma 2}$) Methyl Groups in $^{15}N,^{13}C$- and $^{15}N,^{13}C,^{2}H$-Labeled Proteins

Catherine Zwahlen,[†,‡] Sébastien J. F. Vincent,[†,§,⊥] Kevin H. Gardner,[†] and Lewis E. Kay*[,†]

Contribution from the Protein Engineering Network Centers of Excellence and Departments of Molecular and Medical Genetics, Biochemistry, and Chemistry, University of Toronto, Toronto, Ontario, Canada M5S 1A8, Biochemistry Research, Hospital for Sick Children, Toronto, Ontario, Canada M5G 1X8, and Program in Molecular Biology and Cancer, Samuel Lunenfeld Research Institute, Mount Sinai Hospital, Toronto, Ontario, Canada M5G 1X5

Received December 16, 1997

Abstract: A new NMR experiment is described for recording NOEs from Val and Ile methyl groups in $^{15}N,^{13}C$-labeled or methyl-protonated, $^{15}N,^{13}C,^{2}H$-labeled proteins that offers far superior resolution than conventional 3D ^{13}C-edited NOESY data sets. Resolution is achieved by recording both the C^{β} and C^{γ} (Val) or $C^{\gamma 2}$ (Ile) chemical shifts as well as the chemical shift of the destination proton, and a strategy is introduced for refocusing homonuclear carbon couplings during the constant-time evolution of C^{β} carbon magnetization. The utility of the method is demonstrated with applications on a 160-residue fully protonated $^{15}N,^{13}C$-labeled, dNumb PTB domain−peptide complex and a methyl protonated, highly deuterated $^{15}N,^{13}C$-labeled complex of maltose binding protein and β-cyclodextrin (42 kDa).

Introduction

Protein structure determination by NMR spectroscopy relies on the use of geometrical constraints derived from nuclear Overhauser effect (NOE) intensities,[1] scalar couplings,[2] and more recently dipolar couplings.[3,4] The accurate quantification of these data necessitates recording spectra with high sensitivity and resolution. This is a particularly significant problem in the case of NOE spectroscopy of large macromolecules where the many proximal protons lead to spectra that are often difficult to assign. In this regard the development of double- and triple-resonance multidimensional NMR spectroscopy is an important advance. In addition to recording the chemical shifts of protons which establish the NOE correlation, the shifts of the one-bond-coupled heteroatoms are also measured, resulting in significant resolution gains over the corresponding two-dimensional homonuclear spectra.[5] The power of this methodology has been amply demonstrated by the large number of structures of proteins and protein complexes that have been published in the past several years.[6,7]

Despite the demonstrated utility of multidimensional NOESY spectroscopy, it is still clear that resolution remains a problem. In particular, overlap in the aliphatic−aliphatic region of three- and four-dimensional NMR spectra of even modestly sized proteins (15−20 kDa) can complicate assignment of NOEs critical for structure determination. This includes the methyl−methyl region of NOE spectra, where crucial distance restraints connecting residues comprising the hydrophobic core of the molecule can be difficult to obtain. In the absence of such long-range interactions it is often difficult to build an accurate preliminary structural model to aid in the assignment of subsequent NOE restraints.

With these problems in mind we have developed an experiment for providing NOE correlations linking methyl protons of Val and Ile ($C^{\gamma 2}$) with neighboring spins. Resolution is improved by recording both C^{γ} and C^{β} chemical shifts using a constant-time approach,[8,9] and sensitivity concerns are addressed by recording the $^{13}C^{\beta}$ chemical shift without evolution from one-bond $^{13}C-^{13}C$ scalar couplings. The utility of the experiment is demonstrated on a fully protonated $^{15}N,^{13}C$-labeled sample of a complex of the dNumb PTB domain (160 residues) with a high-affinity-binding peptide (unlabeled) and on a methyl-protonated, $^{15}N,^{13}C,^{2}H$-labeled sample of maltose binding protein (MBP, 370 residues) in complex with β-cyclodextrin.

Materials and Methods

A sample of $^{15}N,^{13}C$-labeled drosophila Numb (dNumb) phosphotyrosine binding (PTB) domain in complex with a high-affinity-binding seven-residue peptide, Ac-AYIGPpYL, where Ac is an acetyl group (A = alanine, Y = tyrosine, I = isoleucine, G = glycine, P = proline, pY = phosphotyrosine, and L = leucine), was prepared as described

[†] University of Toronto.
[‡] Hospital for Sick Children.
[§] Mount Sinai Hospital.
[⊥] Present address: Nestlé Research Center, Vers-chez-les-Blanc, CH-1000 Lausanne 26, Switzerland.

(1) Wüthrich, K. *NMR of Proteins and Nucleic Acids*; John Wiley & Sons: New York, 1986.
(2) Bax, A.; Vuister, G. W.; Grzesiek, S.; Delaglio, F.; Wang, A. C.; Tschudin, R.; Zhu, G. *Methods Enzymol.* **1994**, *239*, 79.
(3) Tolman, J. R.; Flanagan, J. M.; Kennedy, M. A.; Prestegard, J. H. *Proc. Natl. Acad. Sci. U.S.A.* **1995**, *92*, 9279.
(4) Tjandra, N.; Omichinski, J. G.; Gronenborn, A. M.; Clore, G. M.; Bax, A. *Nat. Struct. Biol.* **1997**, *4*, 732.
(5) Bax, A. *Curr. Opin. Struct. Biol.* **1994**, *4*, 738.
(6) Garrett, D. S.; Seok, Y. J.; Liao, D. I.; Peterkofsky, A.; Gronenborn, A. M.; Clore, G. M. *Biochemistry* **1997**, *36*, 2517.
(7) Yu, L.; Petros, A. M.; Schnuchel, A.; Zhong, P.; Severin, J. M.; Walter, K.; Holzman, T. F.; Fesik, S. W. *Nat. Struct. Biol.* **1997**, *4*, 483.
(8) Vuister, G. W.; Bax, A. *J. Magn. Reson.* **1992**, *98*, 428.
(9) Santoro, J.; King, G. C. *J. Magn. Reson.* **1992**, *97*, 202.

S0002-7863(97)04260-1 CCC: $15.00
Published on Web 05/05/1998

previously.[10] Sample conditions were 1.5 mM protein with equimolar peptide, 20 mM sodium phosphate, 150 mM NaCl, 0.1 mM benzamidine, 0.1 mM EDTA, 20 mM deuterated DTT, >99% D_2O, pD 6.0 (uncorrected).

^{15}N,^{13}C,^{2}H,^{1}H-methyl (Val, Leu, and Ile $\delta1$) labeled *Escherichia coli* maltose binding protein was generated by overexpression in *E. coli* grown in D_2O-based M9 minimal medium supplemented with deuterated, site-protonated valine and 2-ketobutyrate.[11] Specifically, *E. coli* strain BL21(DE3) was transformed with plasmid pmal-c_0, which encodes the 370 amino acid residues of mature MBP (preceded by an N-terminal methionine) under the control of a strong, IPTG-inducible promoter. These bacteria were grown overnight at 37 °C on a solid LB/ampicillin medium to generate colonies, one of which was used to inoculate 3 mL of liquid LB/ampicillin medium. After 3 h of growth at 37 °C, this culture was centrifuged briefly to remove the medium, and the cell pellet resuspended in 50 mL of an H_2O-based M9 minimal medium containing $^{15}NH_4Cl$ and [$^{13}C_6$]glucose (Cambridge Isotope Laboratories). This culture was grown for 4 h (to $A_{600} = 0.6$) and centrifuged and the medium replaced with 100 mL of D_2O-based M9 ($^{15}NH_4Cl$ and [$^{13}C_6$,$^{2}H_7$]glucose (CIL)). Note that this procedure resulted in a 100 mL culture with a starting A_{600} of approximately 0.3, higher than the level of $A_{600} \approx 0.1$ that we have previously recommended.[12] We strongly suggest using a D_2O culture with a starting A_{600} of 0.1 to dilute the ^{1}H-labeled bacteria in the deuterium-rich medium (see below).

When this culture reached $A_{600} = 0.6$ (approximately 1.7 h), the medium was removed by centrifugation and replaced with 400 mL of fresh D_2O-based M9 medium ($^{15}NH_4Cl$ and [$^{13}C_6$,$^{2}H_7$]glucose). After 4.5 h, the cell density had reached $A_{600} = 0.5$, and we added an additional 100 mL of D_2O-based M9 medium, supplemented at this point with 25 mg each of (2,3-$^{2}H_2$),^{15}N,^{13}C-labeled valine (CIL) and (3,3-$^{2}H_2$),^{13}C-labeled 2-ketobutyrate[11] as well as $^{15}NH_4Cl$ and [$^{13}C_6$,$^{2}H_7$]-glucose. After an additional hour ($A_{600} = 0.6$), 125 mg of IPTG was added to induce overexpression of MBP. Expression was allowed to continue at 37 °C for 8 h before the bacteria were harvested by centrifugation (see below). MBP was purified from these cells through sequential amylose affinity, ion exchange, and size exclusion chromatography steps for a total yield of over 100 mg of protein/L of medium. To ensure full protonation of the backbone amide groups of MBP, a sample of the protein was incubated for several hours at room temperature in 2.5 M guanidinium hydrochloride (GuHCl) prior to refolding in a GuHCl-free buffer. β-Cyclodextrin was added to a final concentration of 2 mM, and the sample was concentrated using a Centricon 10 concentrator. Final sample conditions were 1.4 mM MBP, 2.0 mM β-cyclodextrin, 20 mM sodium phosphate buffer (pH 7.2), 3 mM NaN_3, 100 μM EDTA, 0.1 mg/mL Pefabloc, 1 μg/μL pepstatin, and 10% D_2O.

As part of the initial characterization of the MBP−β-cyclodextrin complex, 2D $^{13}C-^{1}H$ CT-HSQC spectra[8,9] were acquired. These spectra show that the protonated methyl groups of Val, Leu, and Ile have an isotopic composition of roughly 90% CH_3:10% (CH_2D and CHD_2). These partially deuterated isotopomers were not observed in three previous samples of the MBP−β-cyclodextrin complex that we had generated by diluting cells to an A_{600} of ~0.1 when the H_2O-based medium was replaced with D_2O (see above) and when cultures were induced at lower cell densities ($A_{600} \approx 0.3-0.5$) followed by protein expression for shorter periods of time (3−4 h).[11] In this regard it is noteworthy that other laboratories have obtained excellent results (i.e., no CH_2D and CHD_2 isotopomers) using our previously published protocol.[11] The presence of small (and avoidable) amounts of CH_2D and CHD_2 methyl isotopomers in the MBP sample has led to the development of sequences which can effectively suppress contributions arising from these moieties, as described below.

Chemical shift assignments of the MBP−β-cyclodextrin complex have recently been completed using triple-resonance methods optimized for use on ^{15}N,^{13}C,^{2}H (^{1}H-methyl) labeled samples[13−16] and will be described in detail elsewhere. Stereospecific assignments of the Val and Leu methyl groups were made on the basis of the relative signs of cross-peaks observed in $^{13}C-^{1}H$ CT-HSQC spectra of an ^{15}N,10% ^{13}C-labeled, fully protonated MBP sample complexed with β-cyclodextrin.[17]

NMR experiments on the dNumb PTB domain complex were performed at 30 °C on either a Varian 600 MHz Inova spectrometer (3D Val/Ile (HM)CMCB(CMHM)-NOESY) or a Varian 500 MHz Inova spectrometer (3D ^{13}C-edited NOESY[18]), both equipped with pulsed field gradient units and triple-resonance probes with actively shielded *z* gradients. The 3D ^{13}C-edited NOESY experiment (90 ms mixing time) was recorded as a matrix of 128 × 32 × 384 complex points in each of t_1, t_2, and t_3 with spectral widths of 4200 Hz, 3000 Hz, and 7505 Hz in F_1, F_2, and F_3. Each FID was recorded with 16 scans and a relaxation time of 1 s, resulting in a net acquisition time of 3.5 days. The 3D Val/Ile (HM)CMCB(CMHM)-NOESY experiment was recorded as a data matrix consisting of 58 × 28 × 448 complex points in each of t_1, t_2 and t_3 with spectral widths of $F_1 = 4250$ Hz, $F_2 = 2900$ Hz, and $F_3 = 9000$ Hz. A total of 64 scans/FID were recorded, a delay between scans of 1 s was employed, and a mixing time of 90 ms was used, resulting in a net acquisition time of 5 days.

In the case of MBP, the 3D (HM)CMCB(CMHM)-NOESY data set was recorded at 600 MHz, 37 °C, on the sample described above. A data matrix consisting of 46 × 65 × 512 complex points in each of t_1, t_2, and t_3, and spectral widths of $F_1 = 3400$ Hz, $F_2 = 3600$ Hz, and $F_3 = 9000$ Hz were employed. A mixing time of 100 ms, 32 scans/FID, and a 0.9 s recycle delay were used, resulting in an acquisition time of 120 h.

All spectra were processed using NMRPipe/NMRDraw software[19] and analyzed using the program NMRView.[20] In the case of the 3D ^{13}C-edited NOESY data set linear prediction (forward−backward[21]) was employed to double the t_2 time domain. All dimensions were apodized with 65° shifted squared sine-bell window functions, zero-filled once, Fourier transformed, and phased. The absorptive part of the resulting data set consists of 256 × 128 × 1024 real points.

The t_1 and t_2 time domains of the 3D (HM)CMCB(CMHM)-NOESY data sets recorded on both the dNumb PTB domain and MBP were doubled using mirror image linear prediction[22] according to the procedure described in Kay et al.[23] and discussed by Delaglio et al.[19] Linear prediction was performed in a given dimension only after each of the remaining two dimensions was processed. The acquisition dimension of each experiment was apodized with a 65°-shifted squared sine-bell window function, zero-filled once, Fourier transformed, and phased. In the case of the data set recorded on MBP (H_2O sample) the residual water was removed by a time domain deconvolution of the data at the outset of processing.[24] The data were subsequently processed in F_2 using a sine-bell window function with shifts of 65° and 145° at the start and finish of the time domain without linear prediction but with 1 zero-filling. Subsequently, the t_1 time domain was doubled using mirror image linear prediction, apodized with a Gaussian function (line broadening of 35 and 45 Hz for the PTB domain and MBP, respectively), zero-filled to 256 points, Fourier transformed, and phased, and the imaginaries were eliminated. Finally, the process-

(10) Li, S.-C.; Songyang, Z.; Vincent, S. J. F.; Zwahlen, C.; Wiley: S.; Cantley, L.; Kay, L. E.; Forman-Kay, J. D.; Pawson, T. *Proc. Natl. Acad. Sci. U.S.A.* **1997**, *94*, 7204.

(11) Gardner, K. H.; Kay, L. E. *J. Am. Chem. Soc.* **1997**, *119*, 7599.

(12) Rosen, M. K.; Gardner, K. H.; Willis, R. C.; Parris, W. E.; Pawson, T.; Kay, L. E. *J. Mol. Biol.* **1996**, *263*, 627.

(13) Yamazaki, T.; Lee, W.; Arrowsmith, C. H.; Muhandiram, D. R.; Kay, L. E. *J. Am. Chem. Soc.* **1994**, *116*, 11655.

(14) Yamazaki, T.; Lee, W.; Revington, M.; Mattiello, D. L.; Dahlquist, F. W.; Arrowsmith, C. H.; Kay, L. E. *J. Am. Chem. Soc.* **1994**, *116*, 6464.

(15) Shan, X.; Gardner, K. H.; Muhandiram, D. R.; Rao, N. S.; Arrowsmith, C. H.; Kay, L. E. *J. Am. Chem. Soc.* **1996**, *118*, 6570.

(16) Gardner, K. H.; Konrat, R.; Rosen, M. K.; Kay, L. E. *J. Biomol. NMR* **1996**, *8*, 351.

(17) Neri, D.; Szyperski, T.; Otting, G.; Senn, H.; Wüthrich, K. *Biochemistry* **1989**, *28*, 7510.

(18) Ikura, M.; Kay, L. E.; Tschudin, R.; Bax, A. *J. Magn. Reson.* **1990**, *86*, 204.

(19) Delaglio, F.; Grzesiek, S.; Vuister, G. W.; Zhu, G.; Pfeifer, J.; Bax, A. *J. Biomol. NMR* **1995**, *6*, 277.

(20) Johnson, B. A.; Blevins, R. A. *J. Biomol. NMR* **1994**, *4*, 603.

(21) Zhu, G.; Bax, A. *J. Magn. Reson.* **1992**, *98*, 192.

(22) Zhu, G.; Bax, A. *J. Magn. Reson.* **1990**, *90*, 405.

(23) Kay, L. E.; Ikura, M.; Zhu, G.; Bax, A. *J. Magn. Reson.* **1991**, *91*, 422.

(24) Marion, D.; Ikura, M.; Bax, A. *J. Magn. Reson.* **1989**, *84*, 425.

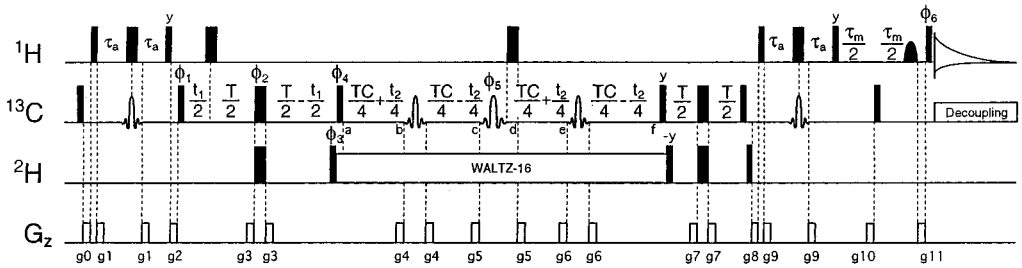

Figure 1. Pulse sequence for the 3D Val/Ile (HM)CMCB(CMHM)-NOESY experiment. All narrow (wide) pulses have flip angles of 90° (180°). ^{1}H and ^{13}C rectangular pulses are centered at 4.73 and 25.0 ppm, and are applied with 30 and 21 kHz fields, respectively. The first and last shaped carbon pulses (INEPT and reverse-INEPT periods) are 1.5 ms IBURP2 inversion pulses[27] centered at 20.5 ppm by phase modulation[36,37] and selectively excite methyl carbons. All three REBURP[27] pulses (points b, c, and e) are centered at 35.6 ppm by phase modulation of the carrier frequency (25 ppm). The pulses at b and e are nonselective, with a duration of 340 μs. The selective REBURP pulse at c is of duration 2.5 ms (600 MHz). For spectra recorded at y MHz (^{1}H frequency) a pulse width of 2.5(600/y) ms should be employed. Applications to ^{15}N,^{13}C-labeled, fully protonated proteins are best performed on samples with ^2H_2O as solvent, so that NOEs to H$^\alpha$ protons are easily observed. In this case, ^{15}N decoupling and all ^{2}H pulses are omitted; the ^{1}H 180° pulse at point d is applied, while the 2 ms water selective pulse applied prior to the end of the NOE mixing period is omitted. The carbon carrier is jumped to 67 ppm prior to acquisition and ^{13}C decoupling achieved using a 4 kHz Garp-1 decoupling field.[38] In the case of applications to methyl-protonated, ^{15}N,^{13}C,^{2}H-labeled proteins the ^{1}H 180° pulse in the center of the TC period is omitted. In this case it is preferable to record spectra on ^1H_2O samples so that NOEs correlating methyl and NH protons are observed as well. A 2 ms water selective pulse is applied prior to the end of the mixing period followed by a homospoil gradient to dephase water that relaxes back to the z-axis during this period. ^{15}N decoupling during acquisition is achieved using a 1 kHz WALTZ-16 field centered at 120 ppm, while ^{13}C decoupling (centered at 20 ppm) employs a 3 kHz WALTZ-16 field.[39] All ^{2}H pulses are centered at 2 ppm and employ a 1.9 kHz field. A 670 Hz field is used for ^{2}H WALTZ-16 decoupling. In the absence of CH_2D and CHD_2 isotopomers the first of the ^{2}H pulses and the last two can be removed and $\phi 3$ set to y. The following delays were used: $2\tau_a = 4.9$ ms, $T = 14.5$ ms $\approx 1/2J_{C\beta CMe}$, and TC = 12 ms (protonated samples), 21.5 ms (methyl-protonated, ^{2}H-labeled samples). The value of TC does not include the length of the REBURP pulse at point c (2.5 ms), and therefore the delays between points a and f are 14.5 and 24 ms for protonated and deuterated samples, respectively. TC can be set to any value since carbon homonuclear couplings involving the C$^\beta$ of Val and Ile are refocused during this interval. Note that $2\tau_a$ is the duration between ^{1}H 90° pulses of the INEPT/reverse-INEPT, and includes the 1.5 ms for the IBURP2 inversion pulse. Evolution due to ^{1}H$-^{13}$C scalar coupling during the IBURP2 pulse (applied simultaneously with the ^{1}H 180° pulse) proceeds at a rate slower than J_{CH}. Quadrature detection in F_1 and F_2 is achieved via States-TPPI[40] of ϕ_1 (F_1) and ϕ_1, ϕ_2, and ϕ_4 (F_2), respectively. The phase cycling employed is $\phi_1 = (x, -x)$; $\phi_2 = x$; $\phi_3 = (y, -y)$; $\phi_4 = 2(y), 2(-y)$; $\phi_5 = 4(x), 4(y), 4(-x), 4(-y)$; $\phi_6 = 8(x), 8(-x), 8(y), 8(-y)$; and rec = $2(x, -x), 4(-x, x), 2(x, -x), 2(y, -y), 4(-y, y), 2(y, -y)$. The duration and strength of the gradients are g_0 = (500 μs, 10 G/cm); g_1 = (400 μs, 5 G/cm); g_2 = (1000 μs, 15 G/cm); g_3 = (200 μs, 18 G/cm); g_4 = (100 μs, 20 G/cm); g_5 = (100 μs, 8 G/cm); g_6 = (100 μs, 30 G/cm); g_7 = (500 μs, 6 G/cm); g_8 = (800 μs, 8 G/cm); g_9 = (200 μs, 7 G/cm); g_{10} = (500 μs, 10 G/cm); and g_{11} = (1000 μs, 7.5 G/cm). The ^{2}H lock channel is interrupted at the start of the sequence and re-engaged at the end of the mixing time.

ing in the F_2 dimension was "undone" and mirror image linear prediction employed to double the t_2 time domain. Apodization in the t_2 dimension of each of the data sets was achieved using Gaussian functions with 65 Hz (PTB) and 35 Hz (MBP) broadening, followed by zero-filling to 128 (PTB) or 256 (MBP) points, Fourier transformation, phasing, and elimination of imaginaries. Note that only those regions of the 3D matrices with NOE cross-peaks were retained at each step of the processing. The digital resolution (Hz/point) in each of F_1, F_2, and F_3 is 16.6, 22.7, and 8.8 and 13.3, 14.1, and 8.8 for the PTB domain and MBP, respectively.

Results and Discussion

NMR Methodology. Figure 1 illustrates the pulse scheme that has been developed to record NOEs linking methyl groups of Val and Ile (C$^{\gamma 2}$) to proximal protons. As discussed below, depending on the ^{13}C$^\gamma$ and ^{13}C$^{\gamma 1}$ chemical shifts of particular Leu and Ile residues, respectively, and the TC delay chosen (Figure 1), it may also be possible to observe NOEs from Leu and Ile ^{13}C$^\delta$ methyls as well. For clarity in the description of the sequence that follows, however, we shall trace the flow of signal from the C$^\gamma$ methyls of either Val or Ile (C$^{\gamma 2}$) and focus initially on applications to proteins which are fully protonated. Magnetization, originating on protons, is transferred by a selective INEPT[25] to the methyl carbon and the carbon chemical shift recorded during a constant-time period, T, which is set to $1/(2J_{CC})$, where J_{CC} is the one-bond aliphatic−aliphatic carbon coupling. The narrow methyl line width ensures that sensitivity losses are minimal during this period. Evolution proceeds due to the one-bond ^{13}C$^\gamma-^{13}$C$^\beta$ coupling so that at the conclusion of the constant-time delay all of the signal is of the form $I^\gamma{}_z C^\gamma{}_x C^\beta{}_z$, where I_i and C_i are the i components of proton and carbon magnetization, respectively. Subsequent application of the ^{13}C 90° pulse of phase $\phi 4$ establishes ^{13}C$^\beta$ magnetization which evolves for the duration of TC. During this period ^{13}C$^\beta$ chemical shift is recorded, and evolution resulting from one-bond ^{13}C$-^{13}$C and ^{13}C$-^1$H couplings must be suppressed.

A number of different strategies are available for refocusing evolution from homonuclear ^{13}C$-^{13}$C scalar couplings. The first approach is based on a scheme introduced by Vuister and Bax[8] and Santoro and King[9] in which the constant time delay, TC, is set to $1/J_{CC}$. In this case the interval between points a and f in Figure 1 is replaced by a sequence of the form t_2/2-180°[^{1}H]-TC/2-180°[^{13}C]-(TC/2 − t_2/2). The magnetization is therefore modulated according to $\cos^n(\pi J_{CC}\mathrm{TC}) = (-1)^n$, where n is the number of ^{13}C spins attached to the C$^\beta$ carbon. A significant limitation of this method results from the long delay ($1/J_{CC} \approx 28$ ms) which must be chosen, leading to unacceptable sensitivity losses in many protein applications. In this regard it is of interest to note that an average ^{13}C$^\alpha$ T_2 value of 14.5 ms was measured for a fully protonated 37 kDa Trp−repressor−DNA complex.[13] For molecules of this size carbon relaxation times at the methine C$^\beta$ positions in Val and Ile residues might be expected to be similar since in many cases these residues are in tightly packed, hydrophobic core regions of proteins.[26]

An alternative strategy for eliminating the $\cos^n(\pi J_{CC}\mathrm{TC})$ intensity modulation is presented in Figure 1. In this case the nonselective ^{13}C refocusing pulses applied at points b and e ensure that evolution due to ^{13}C$-^{13}$C couplings proceeds for both the first (between points a and c) and second (points d−f)

(25) Morris, G. A.; Freeman, R. *J. Am. Chem. Soc.* **1979**, *101*, 760.

(26) Janin, J.; Miller, S.; Chothia, C. *J. Mol. Biol.* **1988**, *204*, 155.

TC/2 periods. However, application of a *selective* ^{13}C refocusing pulse at point c which only affects $^{13}C^{\beta}$ magnetization leads to a net refocusing of $^{13}C-^{13}C$ scalar evolution over the complete interval extending from a to f in the figure. For applications to samples with protonation at the C^{β} position, $^{1}H-^{13}C$ scalar evolution is refocused by the combined action of the ^{1}H and ^{13}C 180° pulses during the constant-time period of duration TC (a−f in Figure 1). Note that the ^{1}H and ^{13}C pulses in the center of this period must not be applied simultaneously, since scalar evolution occurring during the long (2.5 ms) selective ^{13}C refocusing pulse results in significant sensitivity losses.

The flow of magnetization in Figure 1 can be summarized succinctly as

$$^{1}H \xrightarrow{J_{HC}} {}^{13}C^{m}\,(CT\ t_1) \xrightarrow{J_{CC}} {}^{13}C^{\beta}\,(CT\ t_2) \xrightarrow{J_{CC}} {}^{13}C^{m} \xrightarrow{J_{CH}} {}^{1}H^{m} \xrightarrow{NOE} {}^{1}H\ (t_3)$$

where the active couplings involved in each magnetization transfer step are indicated above each arrow and CT t_i is a constant-time evolution period. Fourier transformation of the (t_1, t_2, t_3) data set results in diagonal and cross-peaks at (ω_{Cm}, $\omega_{C\beta}$, ω_{Hm}) and (ω_{Cm}, $\omega_{C\beta}$, ω_{H}), respectively, where ω_{Cm}, $\omega_{C\beta}$, and ω_{Hm} are intraresidue methyl carbon (C^{γ}), β-carbon, and methyl proton chemical shifts and ω_{H} is the resonance frequency of a proton in proximity to the methyl group in question.

In the case of NOE correlations involving pairs of proximal methyl groups from Val or Ile ($C^{\gamma 2}$) residues, symmetry-related peaks are noted on slices corresponding to the $^{13}C^{\beta}$ shifts from residues containing the neighboring methyls, in completely analogous fashion to the observation of symmetry-related cross-peaks for NOEs in standard ^{13}C-edited NOESY data sets. Correlations between methyl groups and non-methyl protons will lack symmetry-related partners, however, since the flow of magnetization is directional in this experiment (i.e., from methyl protons to all other protons). In this regard the Val/Ile NOESY data set is best analyzed in concert with a 3D (4D) ^{13}C-edited NOESY experiment so that in cases where NOEs are to non-methyl protons the identity of these protons can be confirmed.

Figure 2a illustrates the inversion profile of the 2.5 ms REBURP[27] selective pulse (centered at 35.6 ppm) applied at point c in Figure 1, while Figure 2b shows the refocusing profile of transverse magnetization after a four-step cycle of the phase of the pulse. Superimposed on the profile are average chemical shift values (dots) and chemical shift ranges (bars) for Ile (C^{β}, $C^{\gamma 2}$, $C^{\gamma 1}$, C^{δ}), Val (C^{β}, $C^{\gamma 1,2}$), and Leu (C^{γ}, C^{δ}) tabulated from shifts obtained for a number of proteins (see caption of Figure 2). Magnetization within ±0.77 kHz of the center of irradiation of the pulse is inverted ($M_z \rightarrow <-0.98M_z$) while signals outside of a 1.8 kHz window from the center are unaffected ($M_z \rightarrow >0.98M_z$). Thus, for a pulse centered at 35.6 ppm and for spectra recorded at 600 MHz (^{1}H frequency) signals upfield (downfield) of 23.7 ppm (47.5 ppm) are not perturbed. It is noteworthy that for signals which resonate outside a window of ±1.3 kHz from the center of irradiation (<26.8 ppm, >44.4 ppm at 600 MHz) $M_z \rightarrow >0.92M_z$. Numerical simulations of the Bloch equations establish that excellent refocusing of transverse magnetization ($M_{xy} \rightarrow >0.98M_{xy}$) occurs over a bandwidth of ±790 Hz (from 30.3 to 40.8 ppm at 600 MHz) which is sufficient for Ile and Val C^{β} shifts, as Figure 2b illustrates. In the case of spectra recorded at 750 or 800 MHz, a shorter refocusing pulse (2 and 1.875 ms REBURP pulses at 750 and 800 MHz, respectively) is optimal.

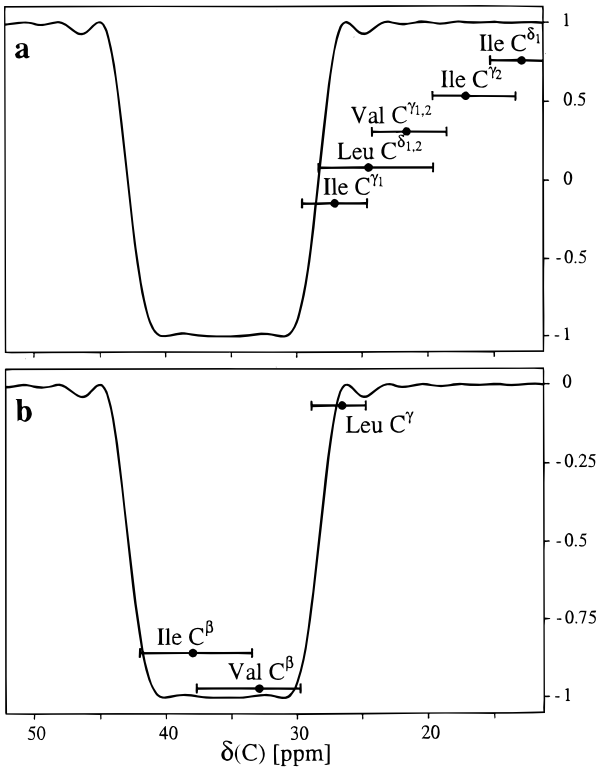

Figure 2. (a) Inversion profile of a 2.5 ms REBURP[27] pulse centered at 35.6 ppm (600 MHz ^{1}H frequency). The average carbon chemical shifts, $^{13}C^{\delta}$ for Leu, $^{13}C^{\delta 1}$, $^{13}C^{\gamma 1}$, and $^{13}C^{\gamma 2}$ for Ile, and $^{13}C^{\gamma}$ for Val, are indicated with dots, with the distribution of shifts illustrated with horizontal lines. (b) Refocusing profile of a 2.5 ms REBURP pulse (at 35.6 ppm) after phase cycling the pulse (x, y, $-x$, $-y$) with concomitant inversion of the receiver phase for every 90° phase shift. The average and distribution of $^{13}C^{\beta}$ chemical shifts for Ile and Val and $^{13}C^{\gamma}$ shifts for Leu are indicated with dots and horizontal lines, respectively. Chemical shifts are based on a database of four proteins, including the C-terminal SH2 domain from phospholipase $C^{\gamma 1}$ complexed with a 12-residue peptide comprising the high-affinity 1021 binding site from the platelet-derived growth factor receptor, staphylococcal nuclease (Ca^{2+} and pdTp),[41] the dNumb PTB domain complexed with a seven-residue peptide, and maltose binding protein with β-cyclodextrin. Average chemical shifts (ppm) are Val C^{β}, 32.9 (37.7, 29.8); Val C^{γ}, 21.6 (24.2, 18.6); Ile C^{β}, 38.0 (42.0, 33.4); Ile $C^{\gamma 1}$, 27.1 (29.6, 24.6); Ile $C^{\gamma 2}$, 17.1 (19.6, 13.3); Ile $C^{\delta 1}$, 12.9 (15.3, 8.7); Leu C^{γ}, 26.5 (28.9, 24.8); and Leu C^{δ}, 24.5 (28.3, 19.6), where the maximum and minimum chemical shift values in the distribution are listed in parentheses. Note that profiles identical to the ones illustrated are obtained at 750 and 800 MHz for REBURP pulses of widths 2 ms (750 MHz) and 1.875 ms (800 MHz).

As described above in the case of protonated proteins, efficient transverse relaxation of magnetization during the TC period limits the duration that can be chosen for this delay and necessarily, therefore, the resolution that is available in the t_2 dimension. Typically, for applications to protonated molecules we set TC ≈ $1/(2J_{CC})$, a compromise between sensitivity losses and resolution. Homonuclear $^{13}C^{\alpha}-^{13}C^{\beta}$ (Val/Ile), $^{13}C^{\beta}-^{13}C^{\gamma}$ (Val), and $^{13}C^{\beta}-^{13}C^{\gamma 2}$ (Ile) couplings are refocused during the TC interval since the selective ^{13}C 180° pulse at point c does not affect $^{13}C^{\alpha}$, $^{13}C^{\gamma}$ (Val), or $^{13}C^{\gamma 2}$ (Ile) spins, but does refocus $^{13}C^{\beta}$ magnetization of Val and Ile residues. For many Ile residues complete or near complete refocusing of the $^{13}C^{\beta}-^{13}C^{\gamma 1}$ coupling occurs as well. Thus, NOE cross-peaks are observed between Val or Ile ($C^{\gamma 2}$) methyls and neighboring

(27) Geen, H.; Freeman, R. *J. Magn. Reson.* **1991**, *93*, 93.

protons. In contrast, correlations between Ile or Leu C^{δ} methyls and proximal protons are seldom observed. In this case magnetization originates on the C^{δ} methyls and is transferred to the C^{γ} carbons for the TC period. As Figure 2 illustrates, in general the $C^{\gamma 1}$ (Ile) and C^{γ} (Leu) chemical shifts fall outside of the window of refocusing of the selective REBURP pulse. Applying the exorcycle to the phase of this pulse ($\phi 5$ in Figure 1) ensures that only magnetization that is refocused is observed in spectra, albeit at a much reduced intensity in the case of residues with chemical shifts that are outside the bandwidth of excitation. In addition, evolution of $C^{\gamma 1}$ (Ile) or C^{γ} (Leu) magnetization due to the $^{13}C^{\gamma 1}-^{13}C^{\beta}$ (Ile) or $^{13}C^{\gamma}-^{13}C^{\beta}$ (Leu) coupling proceeds for the entire TC duration [$\sim 1/2(J_{CC})$], resulting in the generation of antiphase magnetization which is not refocused by the remainder of the pulse scheme.

For applications to Val-, Leu-, and Ile($\delta 1$)-methyl-protonated, $^{15}N,^{13}C,^{2}H$-labeled samples a number of modifications must be made to the pulse scheme, as illustrated in Figure 1. Because all non-methyl carbon positions are highly deuterated, the ^{1}H 180° pulse at the midpoint of the TC period (point d) is no longer required; however, ^{2}H decoupling during this period is essential. For samples containing methyl isotopomers, $^{13}CH_2D$ and/or $^{13}CHD_2$, in addition to the desired $^{13}CH_3$ group, the application of the ^{2}H pulses indicated in Figure 1 suppresses signals from methyls with one or more deuterons, as described in detail by Gardner et al.[28]

One advantage of working with highly deuterated, methyl-protonated samples is that the carbons adjacent to the protonated methyl groups are highly deuterated and thus have significantly longer transverse relaxation times than would be observed in fully protonated molecules. Estimates of $^{13}C^{\beta}$ T_2 values for well-resolved Val cross-peaks in the protein MBP (370 residues) have been obtained from 2D $^{13}C-^{1}H$ correlation spectra in which a spin−echo element is inserted which refocuses evolution from both chemical shift and $^{1}H-^{13}C$ and $^{13}C-^{13}C$ couplings. An average value of 34 ± 10 ms is obtained for a sample in which MBP tumbles with a correlation time of 17.2 ± 0.8 ns, as established by ^{15}N relaxation experiments.[29] We have therefore increased the TC delay in this case to 24 ms, resulting in significantly improved resolution in F_2. An additional advantage of using a TC delay which is set close to $1/J_{CC}$ is that correlations from Leu and Ile residues with downfield $^{13}C^{\gamma}$ (Leu) or $^{13}C^{\gamma 1}$ (Ile) chemical shifts can be observed as long as these shifts are within the refocusing window of the selective REBURP pulse at point c in Figure 1. The majority of these cross-peaks can be readily distinguished from NOEs involving Val by their opposite phase, resulting from the evolution of the $^{13}C^{\gamma}-^{13}C^{\beta}$ (Leu)/$^{13}C^{\gamma 1}-^{13}C^{\beta}$ (Ile) scalar couplings for the duration of the TC period.

Applications to $^{15}N,^{13}C$-Labeled, Protonated Molecules. Figure 3 illustrates the improvements in resolution observed in 3D Val/Ile (HM)CMCB(CMHM)-NOESY spectra of a complex of the dNumb PTB domain and a seven-residue target peptide. In Figure 3a a slice at $F_2 = 21.0$ ppm from the 3D ^{13}C-edited NOESY data set recorded on the complex is shown. Although excellent sensitivity is noted, overlap of the $^{13}C^{\gamma}$ and $^{1}H^{\gamma}$ chemical shifts of Val 91, 131, and 140 renders the assignment of correlations involving the methyls of these residues to unique sites in the molecule close to impossible. In contrast, excellent resolution is noted in slices from the 3D Val/Ile (HM)CMCB-(CMHM)-NOESY data set at F_2 chemical shifts corresponding to the distinct $^{13}C^{\beta}$ resonance positions of these three amino acids (Figure 3b−d). The NOEs observed in this figure, and throughout the data set in general, provide particularly valuable distance restraints between diverse elements of secondary structure in the molecule, defining the overall fold of the protein. For example, in Figure 3b cross-peaks arising from magnetization transfer from Val 91 to Ala 105, Lys 107, Val 108, and Leu 109 define the arrangement of β-strand $\beta 1'$ with respect to α-helix α2. Additionally, the NOE connecting Val 91 and Met 173 links β-strands $\beta 1'$ and $\beta 7$, which make up an antiparallel β-sheet found in other PTB domains as well.[30,31] Figure 3c illustrates correlations connecting Val 131 on the third β-strand, $\beta 3$, with Leu 138 and Lys 136 of the fourth β-strand, $\beta 4$, which is antiparallel to $\beta 3$. Finally, in Figure 3d the NOE between Val 140 and Val 130 links residues on strands $\beta 4$ and $\beta 3$, the NOE to Leu 121 helps position β-strands 2 and 4, and the NOE between Val 140 and His 175 connects $\beta 4$ and $\beta 7$. Figure 4 illustrates correlations from Ile 139 on $\beta 4$ to Val 130 ($\beta 3$) and Val 117 ($\beta 2$). In principle, NOEs between Val and Ile methyls can be assigned unambiguously in the present data set since

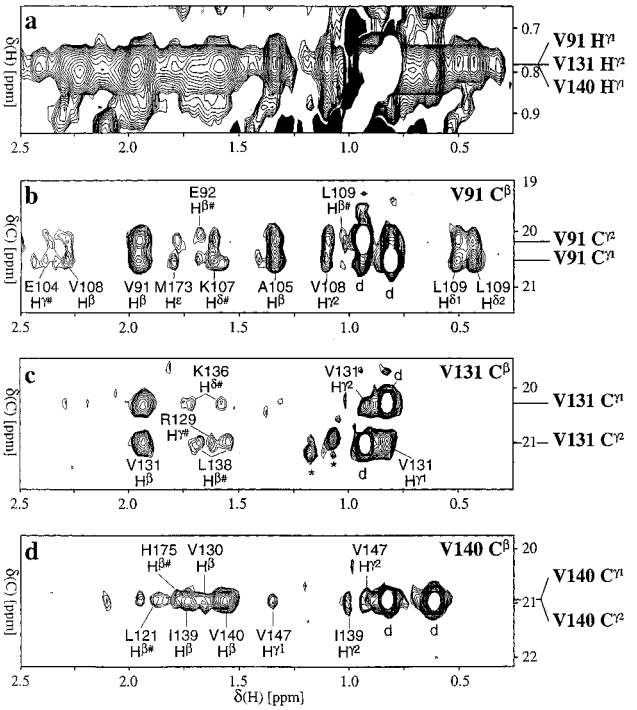

Figure 3. (a) Slice (F_1-F_3) from a 3D ^{13}C-edited NOESY data set ($F_2 = 21.0$ ppm; $\tau_m = 90$ ms) recorded on a 1.5 mM fully protonated, $^{15}N,^{13}C$-labeled dNumb PTB domain in complex with the high-affinity-binding peptide, AcAYIGPpYL (D_2O), illustrating the severe overlap that is common in 3D and 4D ^{13}C-edited data sets obtained from standard pulse schemes. Negative peaks are colored in black. (b−d) Regions from selected planes (F_1-F_3) of the 3D Val/Ile (HM)CMCB-(CMHM)-NOESY experiment ($\tau_m = 90$ ms) recorded on the sample described in (a). Correlations are frequency labeled in F_1 and F_2 by the methyl carbon (C^{γ}) and β-carbon shifts, respectively, (35.6 ppm, 35.0 ppm, and 36.4 ppm for the C^{β} shifts of Val 91, 131, and 140) while the F_3 coordinate provides the proton chemical shift of the site to which magnetization is transferred during the NOE mixing time. NOE cross-peaks from Val 91, 131, and 140 are illustrated in b, c, and d, respectively. Diagonal peaks are labeled with "d", while correlations that are stronger on adjacent slices are indicated by "*".

(28) Gardner, K. H.; Rosen, M. K.; Kay, L. E. *Biochemistry* **1997**, *36*, 1389.

(29) Farrow, N. A.; Muhandiram, R.; Singer, A. U.; Pascal, S. M.; Kay, C. M.; Gish, G.; Shoelson, S. E.; Pawson, T.; Forman-Kay, J. D.; Kay, L. E. *Biochemistry* **1994**, *33*, 5984.

(30) Zhou, M.-M.; Fesik, S. W. *Prog. Biophys. Mol. Biol.* **1995**, *64*, 221.

(31) Zhou, M.-M.; Huang, B.; Olejniczak, E. T.; Meadows, R. P.; Shuker, S. B.; Miyazaki, M.; Trüb, T.; Shoelson, S. E.; Fesik, S. W. *Nat. Struct. Biol.* **1996**, *3*, 388.

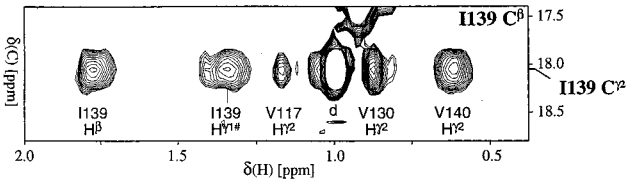

Figure 4. F_1-F_3 slice from the 3D Val/Ile (HM)CMCB(CMHM)-NOESY experiment recorded on the dNumb PTB domain−peptide complex (see caption for Figure 3) at the $^{13}C^{\beta}$ chemical shift of Ile 139 (38.5 ppm).

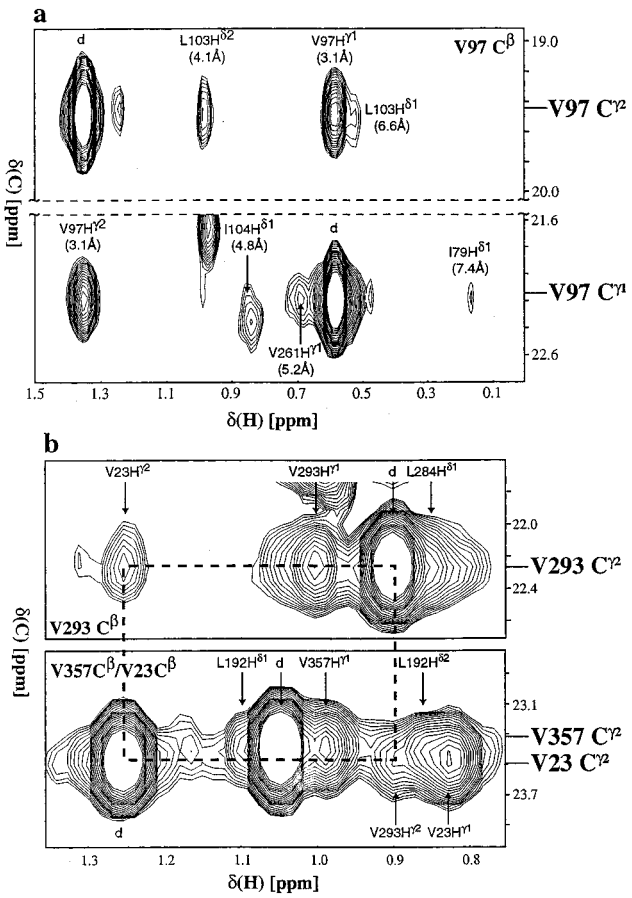

Figure 5. Methyl−methyl NOEs in the MBP−β-cyclodextrin complex identified in F_1 (^{13}C methyl)/F_3 (^{1}H) slices of the (HM)CMCB(CMHM)-NOESY spectrum. (a) Section of an F_1-F_3 slice at the $^{13}C^{\beta}$ chemical shift of Val 97 (30.3 ppm). NOEs are labeled by the identity of the destination methyl group and the distance between pseudoatoms located at the average coordinates of each set of methyl protons, as observed in the 1dmb crystal structure.[33] Diagonal peaks are labeled with "d". (b) Portion of an F_1-F_3 slice at the $^{13}C^{\beta}$ chemical shift of Val 293 (31.5 ppm) [upperframe] and of Val 357 and 23 (both at 31.0 ppm) [lowerframe]. In the lower frame NOEs to Val 357 $H^{\gamma 2}$ are identified above the cross-peaks while those to Val 23 $H^{\gamma 2}$ are identified underneath. A dotted line connects the symmetry-related cross-peaks for the Val 23 $H^{\gamma 2}$−Val 293 $H^{\gamma 2}$ NOE pair.

symmetry-related cross-peaks are often observed. In this regard, the symmetry-related correlations between Ile 139 $H^{\gamma 2}$ and Val 140 $H^{\gamma 2}$ in Figures 3d and 4 are noteworthy.

Applications to Methyl-Protonated, ^{15}N,^{13}C,^{2}H-Labeled Proteins. We have recently developed a biosynthetic scheme where proteins are produced with high levels of deuteration at all positions with the exception of methyl groups of Val, Leu, and Ile ($\delta 1$ only).[11] The narrow methyl line widths[32] and the

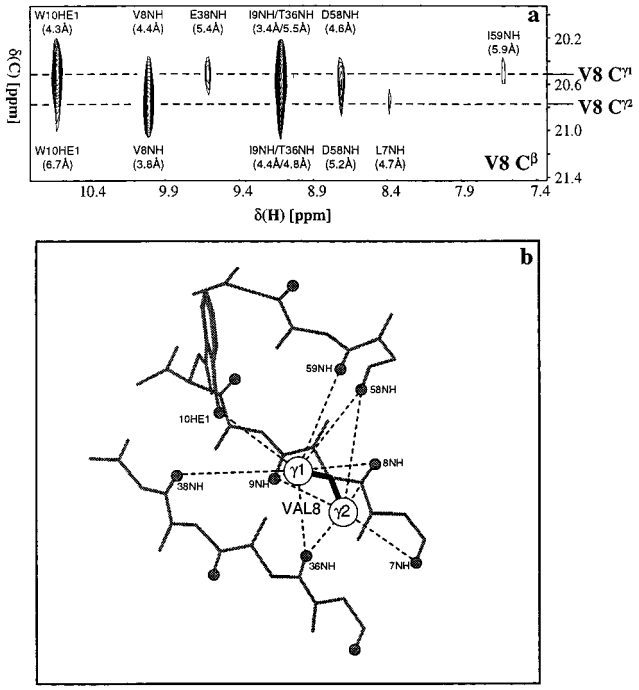

Figure 6. Methyl−NH NOEs in the (HM)CMCB(CMHM)-NOESY spectrum of the MBP−β-cyclodextrin complex. (a) Section of an F_1-F_3 slice at the $^{13}C^{\beta}$ chemical shift of Val 8 (33.3 ppm). NOEs from each of the two C^{γ} methyls are indicated by dashed lines. Assignments and distances (between each amide proton and a methyl pseudoatom as calculated from the 1dmb crystal structure[33]) for each NOE are indicated adjacent to each cross-peak. (b) Schematic diagram of NOEs indicated in (a), using the crystal structure of the MBP−β-cyclodextrin complex (1dmb), modified by rotating the χ_1 dihedral angle of Val 8 from 25° to 176.5°. This view is oriented with the Val 8 $C^{\alpha}-C^{\beta}$ bond toward the viewer, and the side chain of this residue is drawn in thick black lines. The backbone bonds of neighboring residues (and the side chain of Trp 10) are drawn in thinner gray lines and the NH atoms marked by gray circles.

significantly increased ^{13}C relaxation times of carbon spins where one-bond-coupled protons[13] are replaced with deuterons facilitates the use of constant-time spectroscopy to significantly improve spectral resolution, while minimizing sensitivity losses.

Figure 5 demonstrates the quality of NOE data collected on a sample of highly deuterated, methyl-protonated MBP complexed with β-cyclodextrin, using the pulse scheme of Figure 1. NOE cross-peaks correlating methyl groups separated by distances of over 5 Å are observed with high sensitivity, including correlations between $\gamma 1$ methyl groups of Val 97 and Val 261 (5.2 Å; Figure 5a) and between Leu 103 $H^{\delta 1}$ and Val 97 $H^{\gamma 2}$ (6.6 Å) and Ile 79 $H^{\delta 1}$ and Val 97 $H^{\gamma 1}$ (7.4 Å). The NOEs identified in Figure 5a correlate the methyls of five residues with the methyl groups of Val 97. These residues, which are widely dispersed throughout the primary sequence (amino acids 79−261), are located on four different β-strands[33] of two opposing faces of a β-sandwich. It is clear that NOEs to even only a few key methyls can define the relative orientation of secondary structural elements in proteins.

It is important to emphasize that the X-ray-derived structure of the MBP−β-cyclodextrin complex[33] has been used in the assignment of the NOEs listed in Figures 5 and 6. This is in contrast to the assignments presented for the PTB data set, above, where 3D ^{13}C-edited NOESY spectra and the preliminary NMR-derived structure were used in the analysis. As described

(32) Kay, L. E.; Bull, T. E.; Nicholson, L. K.; Griesinger, C.; Schwalbe, H.; Bax, A.; Torchia, D. A. *J. Magn. Reson.* **1992**, *100*, 538.

(33) Sharff, A. J.; Rodseth, L. E.; Quiocho, F. A. *Biochemistry* **1993**, *32*, 10553.

above in the case of NOEs between pairs of Val or Ile methyl groups, the presence of symmetry-related cross-peaks permits, in principle, unambiguous assignment in the absence of additional information. Figure 5b illustrates NOEs between methyl groups of Val 23 γ2 and Val 293 γ2 (3.9 Å separation) of MBP, located on adjacent α-helices that are aligned in an essentially antiparallel manner. The relatively high resolution that is obtained in each of the indirectly detected constant-time carbon dimensions is extremely important for the assignment of NOEs in large proteins, as demonstrated in Figure 5b. Despite the fact that the ^{13}C chemical shifts of Val 23 γ2 and Val 357 γ2 methyl groups are separated by only 0.2 ppm, cross-peaks to each methyl can be distinguished.

The (HM)CMCB(CMHM)-NOESY spectrum of the MBP−β-cyclodextrin complex was recorded on a sample dissolved in H_2O, allowing observation of NOEs between methyl and NH groups. Figure 6a shows NOEs correlating Val 8, located in a parallel β-sheet, with backbone amide protons of residues on adjacent strands of the same sheet (e.g., Thr 36, Glu 38, Asp 58, and Ile 59). In addition, a number of interresidue, intrastrand NOEs are also observed. During analysis of this NOE data an inconsistency with the X-ray-derived structure of the complex of MBP and β-cyclodextrin[33] became apparent. Figure 6a illustrates that an NOE is observed between the Val 8 γ1 methyl group (and not Val 8 γ2) and the amide proton of Glu 38 (backbone) with the NOE connecting Val 8 γ1 and Trp 10 (side chain) stronger than the Val 8 γ2−Trp 10 correlation. Thus, the distances between the γ1 methyl of Val 8 and both of the NH groups of Glu 38 and Trp 10 are less than the corresponding distances involving the γ2 methyl. However, an examination of the crystal structure suggested that exactly the opposite distance relationship should be observed.[33]

A number of different possibilities can account for the disagreement between the NMR- and X-ray-derived results. First, it is noteworthy that stereospecific assignments of the valine methyl groups were established by NMR experiments on the basis of the signs of ^{1}H−^{13}C correlation peaks recorded on a sample of MBP generated from *E. coli* grown on 10% ^{13}C-labeled glucose.[17] It is thus very unlikely that these assignments are incorrect. It may well be the case that there are differences between the structure of MBP in solution and crystalline states. For example, in the crystal form a value of 25° is reported for the Val 8 χ_1 angle. In contrast, the pattern of NOEs observed in solution is consistent with a χ_1 value of approximately 180° (trans conformation). In addition, $^3J_{NC\gamma}$ and $^3J_{COC\gamma}$ coupling constants[2] for this residue also indicate that $\chi_1 \approx 180°$. Figure 6b shows the relative distances between the γ1 and γ2 methyls of Val 8 and proximal NH groups assuming a χ_1 angle of 176.5°. In this figure we illustrate a portion of the X-ray structure with the χ_1 angle of Val 8 modified to its solution value. It is clear from even a qualitative analysis of the NOE intensities in Figure 6a that a χ_1 value of approximately 180° is much more likely than a value of 25°. Finally we note that of the eight MPB crystal structures available in the Brookhaven Protein Data Bank, six have Val 8 in a trans conformation with an average χ_1 value of 176.5° (the two exceptions are 1dmb[33] and 1omp[34]). As well, analysis of backbone-dependent rotamer libraries shows that the trans χ_1 rotamer is observed for approximately 90% of all valines located in β-strands.[35]

Conclusion

A pulse scheme for measuring NOEs from Val/Ile to proximal protons is described. Because both of the indirectly detected dimensions are recorded in constant-time mode, with refocusing of homonuclear carbon couplings, the experiment offers significantly improved resolution relative to other ^{13}C-edited experiments. The utility of the experiment is demonstrated with applications on a fully protonated ^{15}N,^{13}C-labeled sample and a methyl protonated, ^{15}N,^{13}C,^{2}H-labeled complex of 42 kDa. The present pulse scheme is a powerful addition to the existing family of 3D and 4D ^{13}C-edited NOE sequences.

Acknowledgment. This research was supported by grants from the National Cancer Institute of Canada (L.E.K.) and the Medical Research Council of Canada (L.E.K.). The authors thank Professor Kalle Gehring (McGill University) for providing the maltose binding protein plasmid pmal-c_0, Mr. Randall Willis (Hospital for Sick Children) for help with the preparation of the maltose binding protein sample, Drs. S. C. Li and Tony Pawson (Mount Sinai Hospital) for the dNumb PTB sample, and Dr. Ranjith Muhandiram (University of Toronto) for recording the coupling constant data. C.Z. is the recipient of a Human Frontiers Science Program fellowship. S.V. acknowledges a Human Frontiers Science Program long-term fellowship. K.H.G. was supported by a postdoctoral fellowship from the Helen Hey Whitney Foundation. L.E.K. is an International Howard Hughes Research Scholar.

JA9742601

(34) Sharff, A. J.; Rodseth, L. E.; Spurlino, J. C.; Quiocho, F. A. *Biochemistry* **1992**, *31*, 10657.
(35) Dunbrack, R. L., Jr.; Cohen, F. E. *Protein Sci.* **1997**, *6*, 1661.
(36) Boyd, J.; Scoffe, N. *J. Magn. Reson.* **1989**, *85*, 406.
(37) Patt, S. L. *J. Magn. Reson.* **1992**, *96*, 94.
(38) Shaka, A. J.; Barker, P. B.; Freeman, R. *J. Magn. Reson.* **1985**, *64*, 547.
(39) Shaka, A. J.; Keeler, J.; Frenkiel, T.; Freeman, R. *J. Magn. Reson.* **1983**, *52*, 335.
(40) Marion, D.; Ikura, M.; Tschudin, R.; Bax, A. *J. Magn. Reson.* **1989**, *85*, 393.
(41) Baldisseri, D. M.; Pelton, J. G.; Sparks, S. W.; Torchia, D. A. *FEBS Lett.* **1991**, *281*, 33.